

See discussions, stats, and author profiles for this publication at: <https://www.researchgate.net/publication/230785115>

# Effect of Interfacial Hydrogen Bonding on the Freezing/Melting Behavior of Nanoconfined Liquids

ARTICLE in THE JOURNAL OF PHYSICAL CHEMISTRY C · MARCH 2010

Impact Factor: 4.77 · DOI: 10.1021/jp911684m

---

CITATIONS

10

---

READS

26

10 AUTHORS, INCLUDING:



**Dhanadeep Dutta**

Bhabha Atomic Research Centre

56 PUBLICATIONS 380 CITATIONS

SEE PROFILE



**Mayukh Majumder**

Max Planck Institute for Chemical Physics ...

19 PUBLICATIONS 52 CITATIONS

SEE PROFILE



**Bholanath Pahari**

Goa University

31 PUBLICATIONS 188 CITATIONS

SEE PROFILE



**Kajal Ghoshray**

Saha Institute of Nuclear Physics

90 PUBLICATIONS 1,048 CITATIONS

SEE PROFILE

# Effect of Interfacial Hydrogen Bonding on the Freezing/Melting Behavior of Nanoconfined Liquids

P. Maheshwari, D. Dutta, S. K. Sharma, K. Sudarshan, and P. K. Pujari\*

Radiochemistry Division, Bhabha Atomic Research Centre, Mumbai-400 085, India

M. Majumder, B. Pahari, B. Bandyopadhyay, K. Ghoshray, and A. Ghoshray

ECMP Division, Saha Institute of Nuclear Physics, 1/AF, Bidhannagar, Kolkata-400064, India

Received: September 5, 2009; Revised Manuscript Received: February 9, 2010

The effect of interfacial hydrogen bonding on the behavior of the freezing/melting processes in two organic liquids, namely, ethylene glycol  $[(\text{CH}_2\text{OH})_2]$  and isopropanol  $[\text{CH}_3\text{CH}(\text{OH})\text{CH}_3]$ , confined in nanopores of ZSM-5 zeolite has been investigated using the positron annihilation spectroscopy (PAS) and nuclear magnetic resonance (NMR) techniques. Both liquids have intermolecular hydrogen bonding and feel attractive interaction toward the surface of the confining wall, resulting in an increase in the freezing/melting temperature while confined in nanopores. This observation differs from our earlier report on the behavior of benzene confined in ZSM-5 as well as in silica pores wherein a depression in freezing temperature was seen due to a weakly attractive/repulsive interaction between benzene and the pore surface. The measured  $S$  parameter,  $o$ -Ps lifetime, and intensity profiles across the freezing point of ethylene glycol confined in ZSM-5 are seen to be different from those of isopropanol, signifying the difference in the behavior of phase transition in these two liquids under confinement. It is to be noted that, unlike isopropanol, ethylene glycol has strong intramolecular hydrogen bonding. This causes the difference in the fluid–wall interfacial interaction between ethylene glycol and isopropanol within the confinement. The phase-transition behavior of these two confined liquids was also investigated using the NMR technique by studying the spin–spin relaxation time ( $T_2$ ). The  $T_2$  process in ethylene glycol is expressed as a sum of at least two distinct components exhibiting Gaussian decay, whereas in isopropanol,  $T_2$  is expressed as a sum of three components showing Lorentzian decay. The transitions from one component to another were seen to be consistent with the positron annihilation spectroscopic observation.

## 1. Introduction

Fluids confined in pores exhibit unusual features in their freezing/melting behavior, which is mainly due to the contribution of the interfacial surface free energy in the confinement. The surface of a liquid confined in a small pore becomes large as compared to the volume, and hence, the contribution of interfacial surface free energy becomes vital in changing the freezing/melting properties. The change in the freezing/melting temperature  $\Delta T_f$  of a confined liquid/solid in a pore is generally obtained by using classical thermodynamics (Gibbs–Thomson equation)<sup>1</sup>

$$\Delta T_f = T_{\text{pore}} - T_{\text{bulk}} = -\frac{2(\sigma_{\text{SW}} - \sigma_{\text{LW}})T}{H\rho R} \quad (1)$$

where  $\sigma_{\text{SW}}$  and  $\sigma_{\text{LW}}$  are the interfacial free energies per unit area for the solid–wall and liquid–wall interfaces, respectively,  $H$  is the melting enthalpy of the solid,  $\rho$  is its density, and  $R$  is the radius of the confining pore. The above equation shows that the freezing/melting temperature of a liquid inside the pore decreases from the normal equilibrium temperature, when the solid–wall interfacial free energy is higher than the free energy associated with liquid–wall interface, and vice versa. It is

assumed in eq 1 that the size of the solid formed in the pore is sufficiently large so that the material retains its bulk properties for  $H$  and  $\rho$ . However, in the limit of a small and highly inhomogeneous system (nanopores), where (i) the surface-to-pore volume ratio becomes extremely high, (ii) the concept of surface energy is not well-defined, and (iii) the bulk values of melting enthalpy and density of solids may no longer be valid, a deviation is expected from the Gibbs–Thomson equation. In our earlier work, we have reported this deviation in the context of the freezing/melting process of benzene confined in nanopores of ZSM-5 and silica.<sup>2,3</sup> In the nanodomain, it is important to consider the interfacial effects through a description of the confined phase at the molecular level. We have shown in our earlier report that the obtained experimental results were better described by considering that the benzene molecules form small molecular clusters after being frozen in the nanopores, which obviously supports the equation for Lennard–Jones cluster formation in a spherical cavity<sup>3,4</sup>

$$\frac{\Delta T}{T_{\text{bulk}}} = \frac{A'}{R} - \frac{B'}{R^2} \quad (2)$$

where the coefficients  $A'$  and  $B'$  should depend on the degree of anisotropy in the liquid–wall interface and the interaction energy as well as the enthalpy of freezing of the liquid in the nanopores. A deviation from the classical Gibbs–Thomson equation (eq 1) is clearly seen in eq 2.

\* To whom correspondence should be addressed. E-mail: pujari@barc.gov.in.

To explore the effect of pore size and the interaction of the pore wall with confined molecules on their freezing/melting behavior, a variety of experimental studies, such as differential scanning calorimetry,<sup>1,4,5</sup> nuclear magnetic resonance,<sup>1,6</sup> dielectric spectroscopy,<sup>7–9</sup> and neutron scattering,<sup>10,11</sup> have been carried out. All these studies focused on the phase-transition behavior or the crystalline nature of confined molecules inside the small pores below the bulk freezing/melting point. Some authors have simulated the free energy change of confined molecules by considering the fluid–wall Lennard–Jones interaction inside the small pores to understand the phase transition.<sup>7,12,13</sup> However, a clear picture of the contribution of fluid–wall interaction separated from the finite size effect on the freezing/melting properties has not been evolved in any of these studies. It may be due to the reason that the relative contributions of geometrical confinement and the fluid–wall interaction are still difficult to separate. Also, the topology of the confining matrix may play a crucial role in addition to this effect.<sup>14</sup> The present work, therefore, aims at understanding the contribution of only the fluid–wall interaction on the freezing/melting properties of confined liquids. We have used two types of organic liquids, where the nature of hydrogen bonding is different. Hence, the strength of the interaction of the liquid molecules with the confining wall is different, but the topology and the pore size remain identical. We have taken isopropanol [ $\text{CH}_3\text{CH}(\text{OH})\text{CH}_3$ ], which has intermolecular hydrogen bonding and strong attractive interfacial interaction with the pore surface. The other liquid, ethylene glycol [ $(\text{CH}_2\text{OH})_2$ ], on the other hand, experiences both intra- and intermolecular hydrogen bonding, resulting in a reduction in the strength of interfacial interaction toward the surface. We have used ZSM-5 zeolite as the confining system. It comprises three-dimensional porous networks of  $\text{AlO}_4$  and  $\text{SiO}_4$  tetrahedra linked to each other by shared oxygen atoms that form the uniform surface of the void space topology.<sup>15</sup> The oxygen atoms present on the surface of the void space of ZSM-5 enhance the effect of the interfacial hydrogen bonding.

We have combined PAS and NMR experiments to study the behavior of phase changes in ethylene glycol and isopropanol confined in ZSM-5 zeolite. PAS is an *in situ* probe to study the phase-transition behavior of fluid confined in pores. Several studies have been performed so far to investigate the phase transition of the confined materials using PAS.<sup>2,3,16–20</sup> In all these studies, the systematics of formation and decay of the positronium atom is indexed to get information about the phase transition. Positronium (Ps) is formed either as spin-singlet *para*-positronium (*p*-Ps) or as spin-triplet *ortho*-positronium (*o*-Ps) with a ratio of 1:3. The latter, sufficiently long-lived (142 ns) to interact with its surrounding, decays by three-photon mode. However, in the presence of matter, it can seek out an electron of opposite spin from the pore surface and annihilate through the two-photon mode known as pick-off annihilation. When the pores are filled with liquid, the pick-off rate depends on the electron density as well as the effective surface tension of the confined fluid. In addition, if the volume fraction of the pores is high, a significantly larger part of the positron will interact with the liquid (or the solid following freezing), leading to an alteration in the intensity and lifetime of *o*-Ps. Also, the momentum distribution of electrons with which the positron/Ps interact is likely to be modified following phase transition. This can be observed by monitoring the change in the ratio of the number of counts falling in a fixed energy window centered at 511 keV to the total number of counts, known as the *S* parameter in Doppler broadening spectroscopy. Hence, the *o*-Ps pick-off lifetime with its fractional intensity and the Doppler-

broadened *S* parameter are sensitive indices of phase transition in the confined geometry.

NMR spectroscopy is the ideal complementary method for this study. The techniques of NMR have been widely used to monitor the dynamics of fluid molecules trapped in pores or adsorbed on surfaces and the phase-transition behavior of confined fluid molecules.<sup>21–23</sup> In particular, NMR line shape analysis has been used by Dosseh et al to investigate the phase-transition temperature and the nature of the phase of cyclohexane and benzene confined in mesoporous MCM-41 and SBA-15.<sup>1</sup> They have reported the formation of a partial crystalline phase of benzene under confinement. We have made use of the measurement of nuclear spin–spin relaxation time ( $T_2$ ), which is the characteristic time of decay of nuclear magnetization caused by the exchange of energy within the nuclear spin system. The relaxation process is governed by the average distance between spins, which, in a fluid, is determined by the state of mobility of the molecules embodying the spins. In a porous medium, fluid molecules are in various states of compartmentalization owing to the various pore sizes, and their rigidity (mobility) is affected in various degrees by the temperature of the surroundings. If the molecular motion is fast, the effectiveness of spin–spin interaction is diminished owing to the averaging of the spin–spin dipolar interaction, and the resulting  $T_2$  is long. On the other hand, when molecules are rigid, as in the pores whose size is comparable to that of the molecules, or when the temperature is sufficiently low, the averaging is not so effective and  $T_2$  becomes very short.  $T_2$  in the fluid state is about 2–3 orders of magnitude longer than that in the rigid or frozen state, if the pore size is sufficiently large compared to the size of the molecule. If the majority of fluid molecules is in a state of high mobility, the measurement of  $T_2$  yields an exponential decay of magnetization. On the other hand, fluids bound in small pores often exhibit nonexponential decay arising from a combination of different fluid components that are identifiable only by the states of molecular mobilities they are in. Moreover, in the case of relatively rigid molecules, the strong presence of dipolar interaction may also lead to a Gaussian decay. Hence, relaxation time measurement provides a good local probe to study the phase behavior of confined liquids.

## 2. Experimental Section

Commercially available ZSM-5 zeolite ( $\text{SiO}_2/\text{Al}_2\text{O}_3 = 30$ , surface area =  $380 \text{ m}^2 \text{ gm}^{-1}$ , and pore volume =  $0.22 \text{ cm}^3 \text{ gm}^{-1}$ ) and analytical grade ethylene glycol as well as isopropanol were used for the present study. No dehydration of ethylene glycol was carried out. The ZSM-5 zeolite sample was heated at 573 K under vacuum for 7–8 h to remove adsorbed air and moisture. It was cooled to room temperature and a sufficient volume of either ethylene glycol or isopropanol, as the case may be, was injected into the sample (in vacuum) with a syringe so that the entire sample was covered with liquid. The liquid–sample mixture was kept overnight for homogeneous adsorption of liquid into the pores. The sample was then evacuated at room temperature using a rotary pump for 10–15 min to remove the excess liquid/vapor at the bulk surface of the sample. Other details are reported elsewhere.<sup>2</sup>

For low-temperature measurements, the sample along with the source ( $\sim 8 \mu\text{Ci}$  deposited on thin Kapton foil) was mounted on the cold head of an APD closed cycle helium refrigerator. Temperature variation was carried out in 1 K intervals with an accuracy of  $\pm 0.01 \text{ K}$ . Doppler-broadened annihilation radiation measurements were carried out using an HPGe detector having

a resolution of 1.8 keV at a 1332 keV photo peak of  $^{60}\text{Co}$ . The shape parameter, namely, the  $S$  parameter, defined as the ratio of the number of counts falling in a fixed energy window centered at 511 keV to the total number of counts, was evaluated. We have repeated the experiments in different samples (both cooling and heating cycles), and the reproducibility of the data was seen to be good in both of the liquids confined in zeolite.

Positron annihilation lifetime measurements were carried out using  $\text{BaF}_2$  scintillation detectors in a fast-fast coincidence system. The time resolution measured with a  $^{60}\text{Co}$  source was 300 ps, and the time calibration was 25 ps per channel. Data analysis was carried out using the PATFIT program.<sup>24</sup>

Proton NMR studies were carried out at a resonance frequency of 42.53 MHz with a Bruker MSL100 NMR spectrometer at 9.97 kOe using a field-dial controlled Varian V7400 electromagnet. For NMR measurements, all the samples were sealed under an argon atmosphere in glass tubes. A Bruker temperature controller was used to vary the sample temperature. The relaxation time ( $T_2$ ) has been measured by the familiar Hahn-echo method using the pulse sequence  $90^\circ - \tau - 180^\circ$  signal acquisition, which eliminates the effect of magnetic field inhomogeneity on  $T_2$  decay. A  $90^\circ$  pulse length was set at 2.1  $\mu\text{s}$ . The  $\tau$  values were varied between 0.5 and 30 ms. The intensity of the resonance spectrum for a particular component of the fluid in which the nuclear spins experience a certain kind of interaction, is given by

$$I_{2\tau}(i) = I(i) \exp\left(-\frac{2\tau}{T_2(i)}\right)^{m_i} \quad (3)$$

where  $I_{2\tau}(i)$  is the intensity corresponding to the  $i$ th component of the resonance spectrum after a time  $2\tau$  after the  $90^\circ$  pulse and  $m_i$  is 1 for exponential and 2 for Gaussian decay.<sup>25</sup>  $I(i)$  is the fractional intensity of the components having spin-spin relaxation times of  $T_2(i)$ . The total intensity of the spectrum is

$$(I_{2\tau})_{\text{total}} = \sum_i I_{2\tau}(i) \quad (4)$$

### 3. Results and Discussion

**PAS Results.** Positron annihilation lifetime at room temperature in pure ZSM-5 zeolite has been reported by us earlier.<sup>2</sup> In pure ZSM-5, the two distinct long-lived components of  $o$ -Ps have been obtained. The first long-lived component of  $\tau_p = 4.5$  ns with  $I_p = 3.8\%$  corresponds nicely to the  $o$ -Ps annihilation in crystallographic micropores having a radius ( $R$ )  $\sim 0.51$  nm. The other long-lived component of  $\tau_p = 33.4$  ns with  $I_p = 1.3\%$  corresponds to the  $o$ -Ps annihilation in mesopores (defect) with a radius of  $\sim 1.3$  nm inside the matrix (Table 1 in ref 2). In the present study, the Doppler-broadened  $S$  parameter,  $o$ -Ps pick-off lifetime ( $\tau_p$ ), and intensity ( $I_p$ ) are monitored to investigate the phase transition of ethylene glycol and isopropanol confined in ZSM-5 nanopores (both the micro- and the mesopores). The variation in the  $S$  parameter with temperature during cooling and heating cycles for confined ethylene glycol is shown in Figure 1. It is seen that, during the cooling cycle, the  $S$  parameter initially decreases with the decrease in temperature and a sharp discontinuity in the  $S$  parameter is seen at around 270 K. Below 270 K, the  $S$  parameter decreases and a second discontinuity is seen coinciding with the bulk freezing temperature 260 K. In the heating cycle, interestingly, the  $S$  parameter change is

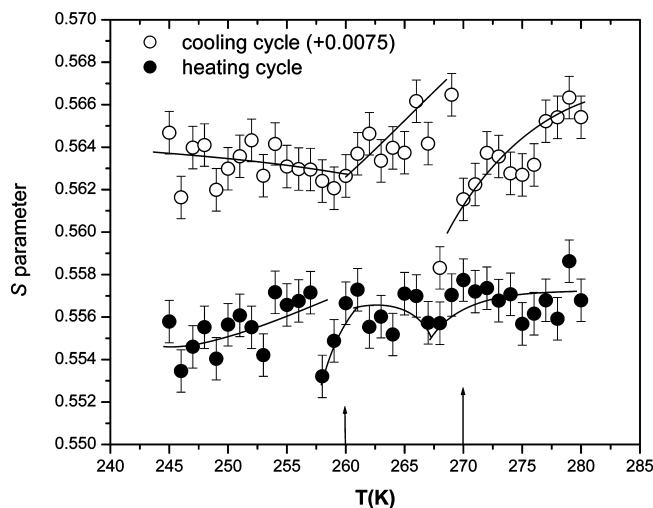


**Figure 1.** Variation in the  $S$  parameter with temperature during cooling and heating cycles for ethylene glycol in ZSM-5. At  $\sim 270$  K, a clear discontinuity (change in slope) representing the pore freezing is seen during the cooling (heating) cycle. The discontinuity at 260 K represents the bulk freezing temperature. The solid lines are a guide to the eye.

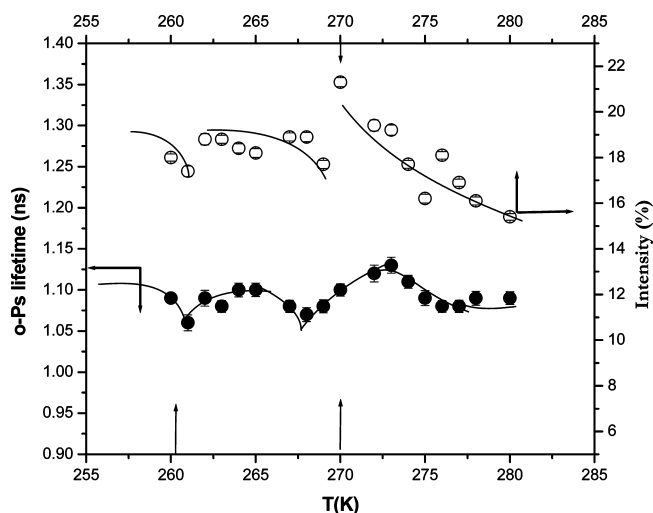


**Figure 2.** Variation in the pick-off lifetime ( $\tau_p$ ) and intensity ( $I_p$ ) during the cooling cycle for ethylene glycol in ZSM-5. At  $\sim 270$  K, a clear indication of phase change above the bulk freezing temperature (260 K) is seen. The solid lines are a guide to the eye.

significant at the bulk freezing temperature and muted at 270 K. The  $o$ -Ps pick-off intensity ( $I_p$ ) and lifetime ( $\tau_p$ ) profile are shown in Figure 2. Both of these parameters show discontinuities at 270 and 260 K during the cooling cycle. The transition at 270 K may be attributed to the freezing of ethylene glycol confined in nanoscopic pores (micropores) of ZSM-5, which is 10 K above the bulk freezing temperature (260 K). However, the values of  $\tau_p$  in Figure 2 remain at about 1.1 ns both in liquid (above 270 K) and in solid (below 260 K) phase, in contrast to the  $\sim 2.3$  ns expected in bulk liquid in this temperature range. This implies either no bubble formation or the volume available for Ps trapping must be similar in either phase. The origin of the available space may be the covolume associated with ethylene glycol molecules. A gross average of  $\sim 26 \times 10^{-3}$  nm<sup>3</sup> for the covolume of a number of organic molecules would result in a lifetime of 1.1 ns, in excellent agreement with the measured  $o$ -Ps lifetime. If the present correlation is correct, then it implies that the confined ethylene glycol molecules (i) are in an arrangement too rigid for Ps to form a bubble and (ii) maintain their covolume over the temperature range studied. The observed



intensity of 15% at 280 K in contrast to 22% in bulk liquid suggests that either a large fraction of positron/Ps are localized in the liquid or there is contribution from the zeolite bulk. However, the role of the solvation phenomenon of electrons in the liquid and its influence on the Ps yield cannot be ignored, as will be discussed later.

The phenomenon of the elevation of freezing point differs from our earlier study on the phase transition of benzene confined in ZSM-5, where a depression of  $\sim 7$  K in freezing temperature of benzene was seen.<sup>2</sup> This shows that the fluid–wall interaction for ethylene glycol in the nanopores of ZSM-5 is different from the case of benzene. For ethylene glycol, this interaction is attractive, whereas it is weakly attractive/repulsive for benzene. The pick-off intensity ( $I_p$ ) response (in Figure 2) is observed to be quite different from the response of the  $S$  parameter (in Figure 1). It is seen that, unlike the  $S$  parameter,  $I_p$  initially increases with the decrease in temperature until the discontinuity at the first phase-transition temperature 270 K. Immediately below 270 K, the  $I_p$  shows a drop at 268 K, which signifies the inhibition of Ps formation after the completion of the liquid-to-solid phase transformation in nanopores. Below 268 K, the  $S$  parameter is seen to decrease slowly until 260 K, which is essentially due to the behavior of liquid trapped in mesopores. At 260 K (bulk freezing point of ethylene glycol), a second discontinuity in  $I_p$ ,  $\tau_p$ , and the  $S$  parameter profile has been observed, which can be ascribed to the freezing of ethylene glycol present in the mesopore and bulk of the ZSM-5 matrix. Below the bulk freezing temperature, the  $S$  parameter does not show any change, at least down to 245 K. Hence, we have not measured  $I_p$  and  $\tau_p$  below the bulk freezing temperature.

One interesting observation (Figures 1 and 2) is the contrasting behavior of the  $S$  parameter and the intensity of  $o$ -Ps. In bulk liquid, upon cooling, the intensity decreases. In general, the  $S$  parameter follows the trend of the intensity. The contrasting behavior observed in the present case, therefore, can be ascribed to possible detrapping of positron/Ps, leading to a broader momentum distribution and concomitant decrease in the  $S$  parameter. However, the role of free positron annihilation in sampling the altered physical state as well as interface cannot be discounted. The behavior of the  $S$  parameter during cooling and heating cycles in isopropanol confined in ZSM-5 is shown in Figure 3. It is seen that the profile of the  $S$  parameter, as well as that of  $I_p$  and  $\tau_p$  (in Figure 4), exhibits a quite different feature from the case in ethylene glycol (Figures 1 and 2). During the cooling cycle, the  $S$  parameter shows a sharp drop near 195 K. The  $I_p$  and  $\tau_p$  profiles also show an abrupt change in the slope in the temperature range of 199–195 K, which illustrates that the phase transition starts near 199 K and continues to 195 K. Below 195 K, the profiles of the  $S$  parameter,  $I_p$ , and  $\tau_p$  show almost constant behavior before the second transition occurs at the bulk freezing point 185 K. It is to be noted that the  $I_p$  is very small (5%) and  $\tau_p$  (2.5 ns) is very close to that of bulk liquid. It was argued that, in the case of ethylene glycol, there could be contribution to  $I_p$  from the zeolite bulk, and a similar contribution should be seen in the case of isopropanol too. However, this seems very unlikely, keeping in mind the low Ps yield. Therefore, solvation of electrons in these liquids can be invoked to explain the yield. It is known that the solvation time in ethylene glycol is very short as compared with isopropanol. In the event of a shallow potential electron trap, the electron can be picked up by the positrons, giving higher Ps yield, a process known as anti-inhibition. In the case of isopropanol, on the other hand, this is not possible due to slower solvation kinetics and, consequently, the yield is

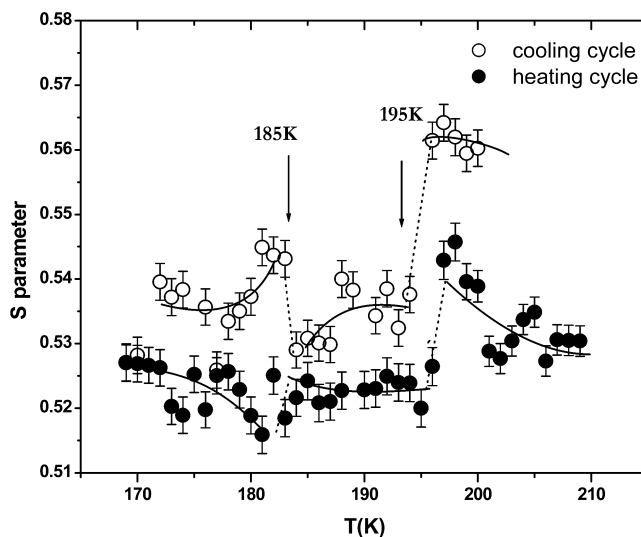


**Figure 3.** Variation in the  $S$  parameter with temperature during cooling and heating cycles for isopropanol in ZSM-5. A sudden drop in the  $S$  parameter at  $\sim 195$  K signifies the pore freezing above the bulk freezing temperature (185 K) during both the cooling and the heating cycles. The solid lines are a guide to the eye.

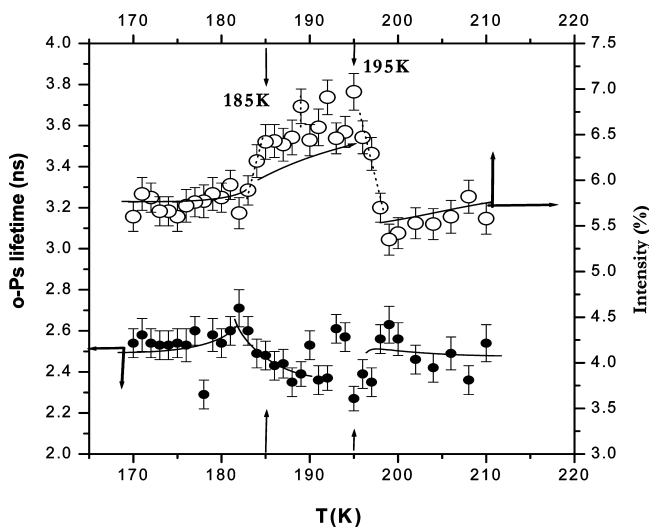


**Figure 4.** Variation in the pick-off lifetime ( $\tau_p$ ) and intensity ( $I_p$ ) during the cooling cycle for isopropanol in ZSM-5. The discontinuity at  $\sim 195$  K above the bulk freezing temperature (185 K) shows the pore freezing. The solid lines are a guide to the eye.

low. Further, the higher lifetime of Ps under confinement indicates that the Ps atom is able to create a hole around itself in the confined isopropanol.

The different behaviors of the  $S$  parameter,  $I_p$ , and  $\tau_p$  signifies that the nature of the phase transition in confined isopropanol is different from the case in ethylene glycol. The major reason behind this dissimilarity is the difference in the nature of hydrogen bonding acting within ethylene glycol and isopropanol molecules, which makes the interfacial interaction different. It is already mentioned that ethylene glycol has both inter- and intramolecular hydrogen bonding, whereas isopropanol has only intermolecular hydrogen bonding. Hence, under confinement, isopropanol experiences more attractive interaction toward the pore wall. This causes the extent of elevation ( $(\Delta T)/(T_{\text{freezing}})$ ) in the phase-transition temperature to be higher in the case of isopropanol. It is observed that the elevation in the phase-transition temperature in ethylene glycol is only 3.8%, whereas in isopropanol, it is around 7.5% relative to their respective bulk

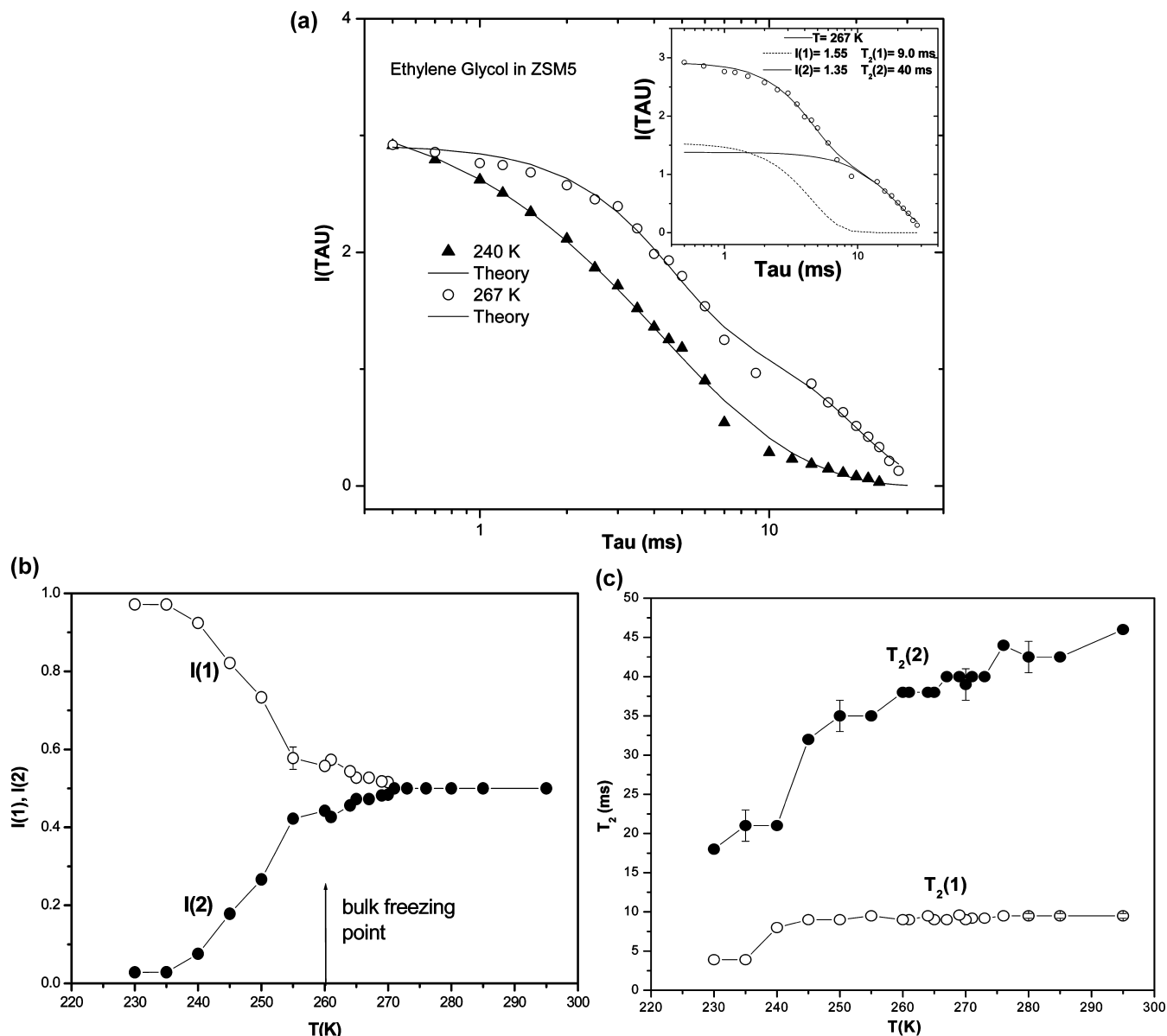


**Figure 5.** (a) Decay of the NMR signal intensity for the  $^1\text{H}$  spin–spin relaxation in ethylene glycol in ZSM-5 at 267 and 240 K. Inset: two distinct fractional intensities ( $I(1)$  and  $I(2)$ ) of the spin–spin relaxation time ( $T_2$ ) are shown at 267 K. (b) Temperature variation of fractional intensities of the molecular components having two different mobilities observed in the  $^1\text{H}$  NMR of ethylene glycol in ZSM-5. (c)  $^1\text{H}$  spin–spin relaxation time ( $T_2$ ) at various temperatures of the molecular components with two different mobilities in ethylene glycol in ZSM-5.

freezing temperature. Although the pore size in both cases remains the same, it is only the distinct interfacial interaction or the surface energy that plays a crucial role to make the phase-transition behavior quite different. In isopropanol, as the molecules strongly interact with the pore surface, the mobility of the molecules near the pore surface decreases very fast with the decrease in temperature. This may also be one of the reasons that manifests differently in the  $S$  parameter,  $\tau_p$ , and  $I_p$  across the phase-transition temperature. The nature of the shift in the phase-transition temperature of ethylene glycol and isopropanol is seen to be different from our earlier observation on benzene confined in ZSM-5, as well as in silica.<sup>2,3</sup> In the case of confined benzene, the phase-transition temperature reduces from the bulk freezing point, unlike ethylene glycol and isopropanol. The reverse trend of shifting clearly manifests that the interfacial interaction of ethylene glycol and isopropanol with the pore surface is different from the case of benzene, as discussed earlier.

**NMR Results.** Figures 5 and 6 present the NMR result originating from the protons of the molecules confined primarily

in the nanopores. Figure 5a shows typical decay curves for ethylene glycol in ZSM-5 taken at 267 and 240 K. In the temperature range of 230–300 K,  $T_2$  decay is expressed as a sum of at least two distinct components exhibiting Gaussian decay. As a typical example, the deconvolution into two components ( $I(1)$  and  $I(2)$ ) for the 267 K decay curve is shown in the inset. The characteristic time for the  $I(1)$  component is in the range of 5 ms and that of the  $I(2)$  component is around 30 ms, with a decreasing trend with decrease in temperature. Considering the values of the time constant, we believe that both of the components are in the fluid state, however with different physical environments. We ascribe the shorter  $T_2(1)$  (Figure 5c) component to fluid molecules directly attached to the pore wall. The molecules away from the pore walls would exhibit a relatively longer  $T_2(2)$  because of the higher mobility like bulk fluid. The  $T_2(1)$  is almost temperature-independent. The gradual decrement in  $T_2(2)$  is due to slowing down of the motion due to lowering of the temperature. The two components are present at about equal intensities at room temperature and

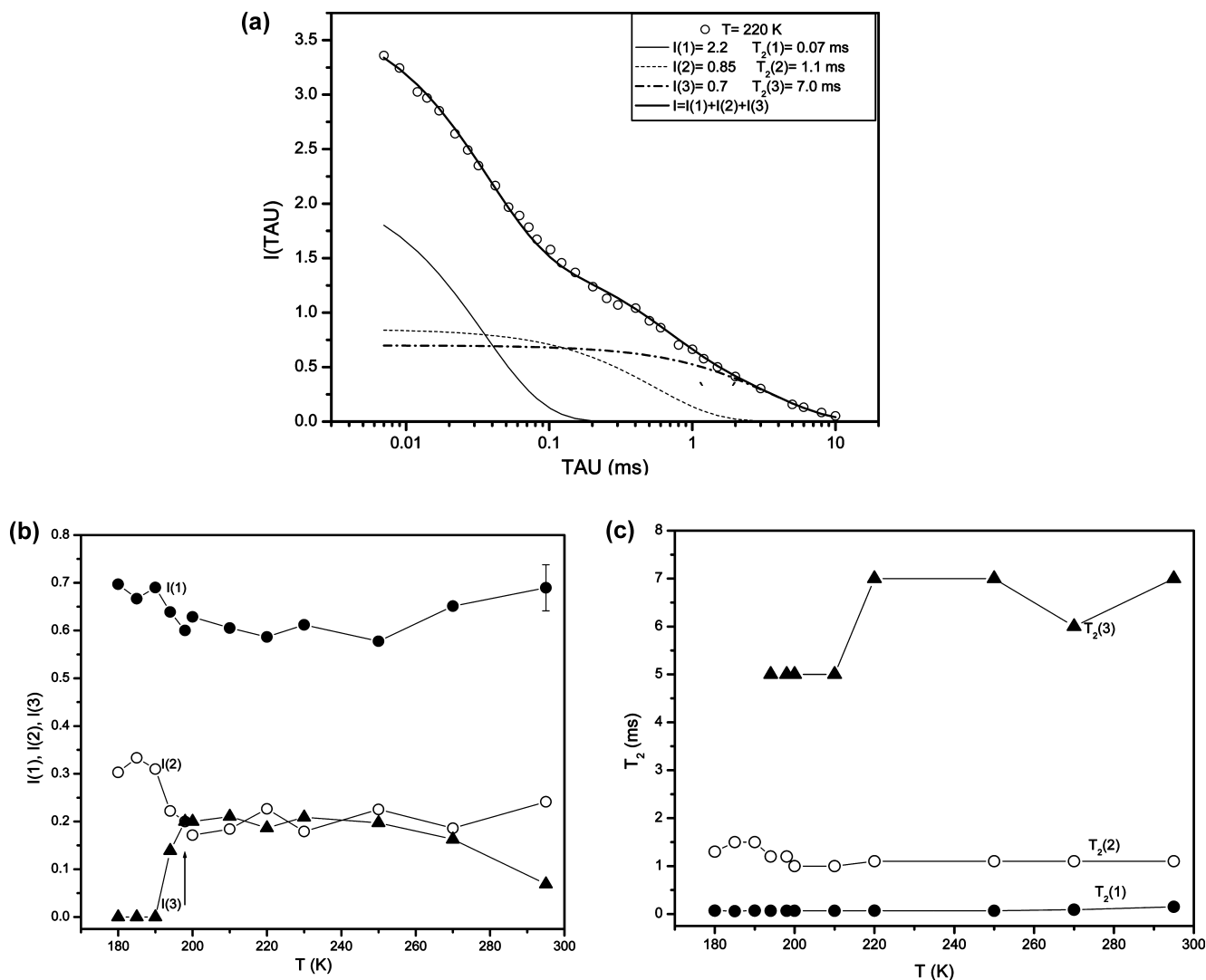


**Figure 6.** (a) Decay of the NMR signal intensity for the  $^1\text{H}$  spin–spin relaxation in isopropanol at 220 K. (b) Temperature variation in fractional intensities of the molecular components with three different mobilities observed in the  $^1\text{H}$  NMR of isopropanol in ZSM-5. (c)  $^1\text{H}$  spin–spin relaxation time ( $T_2$ ) at various temperatures of the molecular components with three different mobilities in isopropanol in ZSM-5.

down to about 270 K. Below this temperature (similar discontinuity in the  $S$  parameter), the intensity of the component with the shorter  $T_2$  begins to increase at the expense of the other component, indicating a transition from a higher to a lower mobility state. This means that fluid pore wall surface interaction starts to percolate toward the center of the pore, facilitating the gradual increase in the number of molecules interacting with the pore wall. This process continues down to 260 K (bulk freezing point of ethylene glycol). From 260 K, the intensity of the component with the shorter  $T_2$  ( $I(1)$  component) starts to dominate, and finally around 235 K, the  $I(2)$  component, that is, that with the longer  $T_2$ , reduces to 10% of the total intensity of the resonance line. Figure 5b,c shows the temperature dependence of the fractional intensities of the two components and their characteristic times.

The shorter  $T_2$  component, as explained before, indicates the presence of strong surface bonded molecules. The other component having a longer  $T_2$  shows the existence of molecules free to move, but still close enough to the surface so that the surface interaction becomes dominant at about 10 K above the bulk freezing point, when the molecular motion is slowed down. It may be said that the part of adsorbed ethylene glycol that exhibits fluidity at room temperature experiences a gradual decrease in mobility below 270 K. Probably, the high degree

of compartmentalization prevents the occurrence of a long-range crystalline order at a sharply defined temperature as it happens in a bulk fluid. A possible reason for this could be the pore size in the present case (0.5–1.3 nm), which is comparable to the molecular size and much smaller compared with other porous materials with a larger pore size (6–50 nm) where definite signature of the crystalline state was observed upon freezing.<sup>22</sup>

In the case of isopropanol in ZSM-5, the  $T_2$  decay at the temperature range of 295–200 K could be satisfactorily expressed as a sum of three components exhibiting Lorentzian decay. Figure 6a shows a typical example of one such fitting at 220 K. The temperature dependence of the fitting parameters,  $I(i)$  and  $T_2(i)$ , is shown in Figure 6b,c. The values of  $T_2$ , which are about 0.07, 1.0, and 5.0 ms, do not show appreciable change with temperature. The component having the shortest  $T_2$  remains dominant, at about 70%, throughout the temperature range. This component indicates the presence of isopropanol molecules rigidly bonded inside the pores through strong surface interaction. The component having such a small value of  $T_2$  has not been seen in ethylene glycol, signifying weaker interaction of ethylene glycol with the pore surface. The intermediate and long components of  $T_2$  in isopropanol signify the presence of molecules having relatively high mobility. Below about 200 K, the component with the longest  $T_2$  is gradually diminished, and

no longer obtained below 190 K, which is indicative of gradual freezing of molecular mobility or a phase transition of molecules away from the pore surface.

PAS and NMR measurements thus explore the nature of the phase transition of two liquids having different liquid–substrate interfacial interaction within the confinement. The structures of the quasi-solid state of ethylene glycol and isopropanol at, near, or below their bulk freezing temperatures thus depend on the relative strength of the interaction within the molecules as well as between the molecules and the pore wall. As discussed earlier, the oxygen atoms present on the surface of the void space of ZSM-5 enhance the effect of the interfacial hydrogen bonding, which provides a strong spatial correlation and supports the propagation of surface-induced order to the molecules at the center of the pore. The fluid molecules having strong interaction with the surface of the pore are generally arranged in a layer structure.<sup>14,25</sup> Hence, the present situation facilitates the layer-like configuration of strongly hydrogen bonded molecules, such as isopropanol. The ethylene glycol, on the other hand, which shows comparatively weaker interfacial hydrogen bonding due to the presence of strong intramolecular hydrogen bonding, is expected to have inhomogeneous phases with a globular structure, as observed in the case of benzene in silica pores.<sup>3</sup> An inhomogeneous phase with a partial crystalline domain is also reported by Radhakrishnan et al. and Bartkowiak et al. using the Monte Carlo simulation method in the context of freezing of nitrobenzene in silica.<sup>7,13</sup> Further, it will be interesting to examine the theoretically predicted qualitative behavior of freezing by taking into account the ratio of fluid–wall to fluid–fluid attractive interactions in confined systems.<sup>26</sup>

#### 4. Conclusion

The effect of interfacial hydrogen bonding on the dynamics of freezing/melting has been explained. An elevation in the freezing temperature is seen in both of the liquids, which can be ascribed to the attractive interaction to the surface through hydrogen bonding. The liquid with both intra- and intermolecular hydrogen bonding (ethylene glycol) showed a smaller relative increase due to weaker interaction as compared with isopropanol. Further studies are required to explore quantitatively the

contribution of structural imperfection and hence the heterogeneity of interfacial energy in nanoscopic scale.

#### References and Notes

- (1) Dosseh, G.; Xia, Y.; Alba-Simionesco, C. *J. Phys. Chem. B* **2003**, *107*, 6445.
- (2) Dutta, D.; Sachdeva, A.; Pujari, P. K. *Chem. Phys. Lett.* **2006**, *432*, 116.
- (3) Dutta, D.; Pujari, P. K.; Sudarshan, K.; Sharma, S. K. *J. Phys. Chem. C* **2008**, *112*, 19055.
- (4) Jackson, C. L.; McKenna, G. B. *J. Chem. Phys.* **1990**, *93*, 9002, and references therein.
- (5) Zheng, W.; Sindee, L. S. *J. Chem. Phys.* **2007**, *127*, 194501.
- (6) Kimmich, R. *Chem. Phys.* **2002**, *284*, 253.
- (7) Sliwinska-Bartkowiak, M.; Dudziak, G.; Sikorski, R.; Gras, R.; Radhakrishnan, R.; Gubbins, K. E. *J. Chem. Phys.* **2001**, *114*, 950.
- (8) Barut, G.; Pissis, P.; Plester, R.; Nimtz, G. *Phys. Rev. Lett.* **1998**, *80*, 3543.
- (9) Gorbatschow, W.; Arndt, M.; Stannarius, R.; Kremer, F. *Europhys. Lett.* **1996**, *35*, 719.
- (10) Schonhals, A.; Goering, H.; Schick, C.; Frick, B.; Zorn, R. *Eur. Phys. J. E* **2003**, *12*, 173.
- (11) Alba-Simionesco, C.; Dosseh, G.; Dumont, E.; Geil, B.; Morineau, D.; Frick, B.; Teboul, V.; Xia, Y. *Eur. Phys. J. E* **2003**, *12*, 19.
- (12) Miyahara, M.; Gubbins, K. J. *Chem. Phys.* **1997**, *106*, 2865.
- (13) Radhakrishnan, R.; Gubbins, K. E.; Sliwinska-Bartkowiak, M. *J. Chem. Phys.* **2000**, *112*, 11048.
- (14) Morineau, D.; Alba-Simionesco, C. *J. Chem. Phys.* **2003**, *118*, 9389.
- (15) Turro, N. J. In *Molecular Dynamics in Restricted Geometries*; Klafter, J., Drake, J. M., Eds.; John Wiley & Sons: New York, 1989; pp 387–404.
- (16) Duffy, J. A.; Wilkinson, N. J.; Fretwell, H. M.; Alam, M. A. *J. Phys.: Condens. Matter* **1995**, *7*, L27.
- (17) Duffy, J. A.; Wilkinson, N. J.; Fretwell, H. M.; Alam, M. A.; Evans, R. *J. Phys.: Condens. Matter* **1995**, *7*, L713.
- (18) Alam, M. A.; Clarke, A. P.; Duffy, J. A. *Langmuir* **2000**, *16*, 7551.
- (19) Duffy, J. A.; Alam, M. A. *Langmuir* **2000**, *16*, 9513.
- (20) Kilburn, D.; Sokol, P. E.; Alam, M. A. *Appl. Phys. Lett.* **2008**, *92*, 033109.
- (21) Strange, J. H.; Rahman, M.; Smith, E. G. *Phys. Rev. Lett.* **1993**, *71*, 3589.
- (22) Gussoni, M.; et al. *Magn. Reson. Imaging* **2004**, *22*, 877.
- (23) Kumagai, H.; et al. In *Structure and Thermoplasticity of Coal*; Komaki, I., et al., Eds.; Nova Science Publishers: New York, 2005.
- (24) Kirkegaard, P.; Pedersen, N. J.; Eldrup, M. *PATFIT-88, Risø-M-2740*; Risø National Laboratory: Roskilde, Denmark, 1989.
- (25) Abragam, A. *The Principles of Nuclear Magnetism*; Clarendon Press: Oxford, U.K., 1961.
- (26) Radhakrishnan, R.; Gubbins, K. E.; Sliwinska-Bartkowiak, M. *J. Chem. Phys.* **2002**, *116*, 1147.

JP911684M